analytical chemistry

Article

pubs.acs.org/ac

Self-Catalytic Growth of Unmodified Gold Nanoparticles as Conductive Bridges Mediated Gap-Electrical Signal Transduction for DNA Hybridization Detection

Jing Zhang,[†] Huagui Nie,*[,†] Zhan Wu,[‡] Zhi Yang,[†] Lijie Zhang,[†] Xiangju Xu,[†] and Shaoming Huang*[,†]

[†]Nanomaterials and Chemistry Key Laboratory, College of Chemistry and Chemical Engineering, Wenzhou University, Wenzhou, Zhejiang 325027, People's Republic of China

[‡]State Key Laboratory of Chemo/Bio-Sensing and Chemometrics, College of Chemistry and Chemical Engineering, Hunan University, Changsha, Hunan 410082, People's Republic of China

S *Supporting Information*

ABSTRACT: A simple and sensitive gap-electrical biosensor based on self-catalytic growth of unmodified gold nanoparticles (AuNPs) as conductive bridges has been developed for amplifying DNA hybridization events. In this strategy, the signal amplification degree of such conductive bridges is closely related to the variation of the glucose oxidase (GOx)-like catalytic activity of AuNPs upon interaction with single- and double-stranded DNA (ssDNA and dsDNA), respectively. In the presence of target DNA, the obtained dsDNA product cannot adsorb onto the surface of AuNPs due to electrostatic interaction, which makes the unmodified AuNPs exhibit excellent GOx-like catalytic activity. Such catalytic activity can enlarge the diameters of AuNPs in the glucose and $HAuCl_4$ solution and result in a connection between most of the AuNPs and a conductive gold film formation with a dramatically increased conductance. For the control sample, the catalytic activity sites of AuNPs are fully blocked by ssDNA due to the noncovalent interaction between nucleotide bases and AuNPs. Thus, the growth of the assembled AuNPs will not happen and the conductance between microelectrodes will be not changed. Under the optimal experimental conditions, the developed strategy exhibited a sensitive response to target DNA with a high signal-to-noise ratio. Moreover, this strategy was also demonstrated to provide excellent differentiation ability for single-nucleotide polymorphism. Such performances indicated the great potential of this label-free electrical strategy for clinical diagnostics and genetic analysis under real biological sample separation.

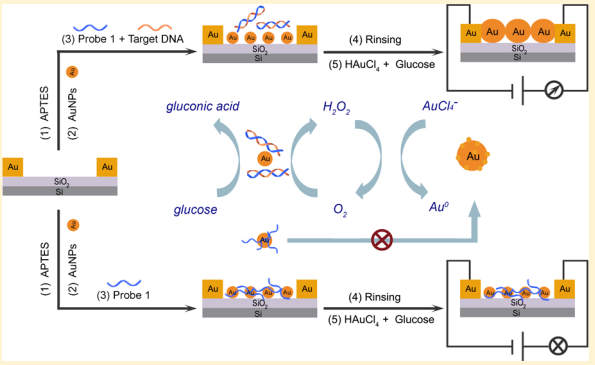

Ever-growing interests in genomics and clinical diagnostics have promoted the development of efficient tools for sensitive assay of low-abundant DNA biomarkers.[1,2] Recently, polymerase chain reaction (PCR) coupled with fluorescence spectroscopy has been viewed as the most widely used technique for sensitive detection of DNA.[3,4] Although with high sensitivity, the PCR-based techniques for DNA detection encounter the problems of complicated procedures, easy contamination, and high cost. Gap-based electrical biosensors devices can provide a viable alternative route to PCR for the rapid quantification of DNA, attributing that such devices can directly transduce nucleic acid hybridization events into useful electrical signals through pairs of microgapped or nanogapped electrodes.[5] These unique properties, coupled with their compatibility with advanced semiconductor technology and large-scale reproducible fabrication and miniaturization, make them very promising in the development of high-performance DNA detection strategies. Especially, with the development of nanotechnology, nanomaterials-based gap-electrical biosensors have been popularly proposed for low-concentration DNA analysis.[6]

Gold nanoparticles (AuNPs) are suitable potential candidate nanomaterials for the sensitive electrical transduction of different biomolecular recognition events due to their attractive electrical properties, excellent biocompatibility, and the availability of versatile bioconjugation means.[7] One of the most representative developments is Mirkin's DNA detection strategy, in which DNA-functionalized AuNPs could be captured in the insulative gap by the hybridization of target DNA, followed by silver enhancement induced by AuNPs.[8] Successful applications of this technique have been demonstrated in a variety of bioassays with a further extension of biobarcode technology.[9,10] However, the unspecific deposition of silver onto the insulative gap in these techniques can significantly improve the background response and even lead to false-positive signals. In order to solve this problem, several groups resorted to aggregated nanoparticles through parent–

Received: October 10, 2013
Accepted: December 9, 2013
Published: December 9, 2013

   dx.doi.org/10.1021/ac4032675 | *Anal. Chem.* 2014, 86, 1178–1185

son AuNPs or Zr ion induced AuNPs aggregation array.[11,12] These strategies can heavily enhance the analyte-specific determination; however, the preparation processes of DNA–AuNPs bioconjugates based on gold–sulfur chemistry were complicated and tedious. An alternative routine for the target DNA gap-electrical identification is to utilize in situ seeded growth of AuNPs for modulating the size of nanogap devices, which may be one of the cheapest and most convenient methods to obtain a size-controllable nanogap device.[13,14] Despite the considerable advances, there has been relatively limited progress toward simultaneous high sensitivity, selectivity, and ease of operation for the trace DNA biomarkers analysis. Hence, it is of considerable interest to exploit a novel intrinsic property of AuNPs for developing a gap-electrical strategy for circumventing the potential problems in the DNA hybridization detection. Very recently, the Fan group found that solution-phase unmodified AuNPs exhibited similar catalytic activity of glucose oxidase (GOx), and such catalytic activity of AuNPs could be finely regulated by DNA hybridization, providing a colorimetric DNA quantitative detection.[15,16] However, this colorimetric method provided limited sensitivity. Considering the unique catalytic activity of AuNPs and the sensitivity of gap-electrical DNA biosensors, hence, applying such novel property of AuNPs in the gap-electrical DNA biosensors devices may be highly desired to produce a highly efficient signal amplification strategy for trace amounts of DNA biomarkers analysis. To the best of our knowledge, research into this area has been still rare so far.

Herein, we developed a novel label-free gap-electrical biosensor strategy based on self-catalytic growth of unmodified AuNPs as conductive bridges mediated electrical signal transduction for DNA hybridization detection. In this strategy, the presence of target DNA can mediate the variation of the GOx-like catalytic activity of AuNPs assembled onto the insulative gaps, attributing to the different electrostatic interactions between AuNPs and single-stranded (ssDNA) and double-stranded (dsDNA), respectively.[17−19] Such catalytic activity can induce the growth of AuNPs in the glucose and $HAuCl_4$ solution, resulting in a dramatic alteration for the conductance between the microelectrodes. This developed label-free electrical strategy seems to be easily executable because there is no requirement of covalent modification of DNA and AuNPs surfaces. Moreover, this strategy can eliminate the second hybridization with a nanoparticles-labeled probe. We demonstrated that this signal transduction strategy based on enlarging surface-assembled AuNPs as conductive bridges can be applied for trace DNA biomarkers detection with high sensitivity and specificity.

EXPERIMENTAL SECTION

Materials and Reagents. All of the DNA oligonucleotides were purchased from Takara Biotech. Co. Ltd. (Dalian, China), and their sequences are listed in Table 1. (3-Aminopropyl)-triethoxysilane (APTES), β-D-glucose, chloroauric acid ($HAuCl_4$), and trisodium citrate were provided from Sigma-Aldrich and used as received. Other reagents and chemicals were all of analytical reagent grade. Ultrapure water with an electrical resistance of >18.2 MΩ was supplied through a Millipore Milli-Q water purification system (Billerica, MA, U.S.A.).

Synthesis of Gold Nanoparticles. The preparation of gold nanoparticles (AuNPs) was adapted from a reported citrate reduction and stabilization of $HAuCl_4$ method with

Table 1. Sequences of Oligonucleotides (5′→ 3′) Used in the Experiments[a]

probe 1	CCACATCATCCATATAGCT
probe 2	AGCTATATGGATGATGTGG
probe 3	AGCTATATGGATGAAGTGG
probe 4	AGCTATGTGGATGAAGTGG
probe 5	ATACAGACTCCGAGACGGAAAACAGACTCCGAGACGGAATACAGACTCCGAGACGAAAACAGACTCCGAGACGGAAAACAGACTCCGAGACGGTTGCGT

[a]Probe **1** is capture probe, which is used as hybridizing with perfectly matched target DNA. Probe **2** is perfectly matched target DNA. Probe **3** is one-base mismatched DNA. Probe **4** is two-base mismatched DNA. Probe **5** is noncomplementary DNA.

dx.doi.org/10.1021/ac4032675 | Anal. Chem. 2014, 86, 1178−1185

Scheme 1. Schematic Diagram of the Gap-Electrical Biosensor Strategy Based on Self-Catalytic Growth of Unmodified AuNPs as Conductive Bridges for DNA Hybridization Detection

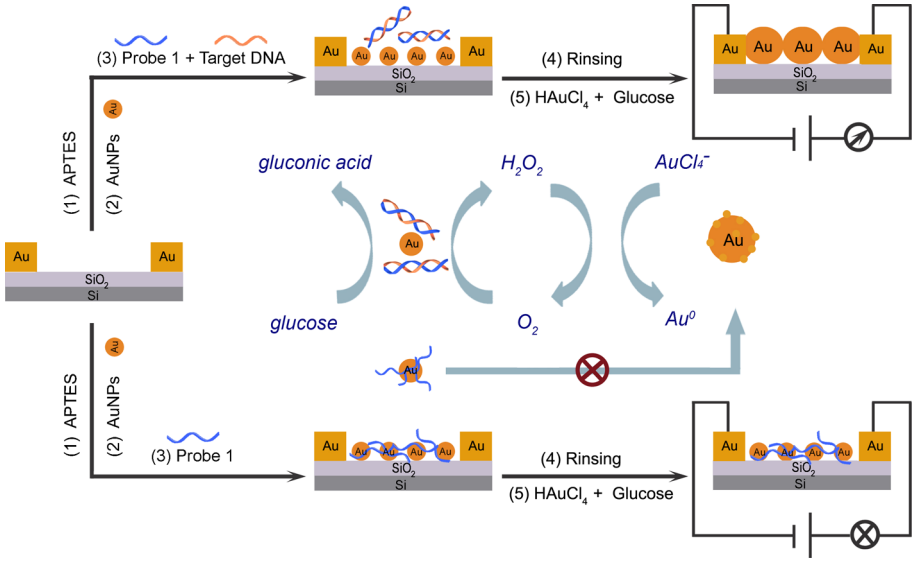

minor modifications,[20] as described briefly as follows. Trisodium citrate (5 mL, 38.8 mM) was rapidly added to a stirred boiling $HAuCl_4$ (220 mL, 1 mM) solution. After several minutes, the color of the solution changed from pale yellow to deep red. Subsequently, the obtained solution was further heated under reflux for another 30 min to ensure complete reduction followed by slow cooling to room temperature. Transmission electron microscopy (TEM, JEOL, Japan) was used to characterize the size and morphology of the synthesized AuNPs. Absorption spectra were obtained from a UV 3600 UV−vis absorption spectrophotometer (Shimadzu, Japan). The obtained AuNPs solution was stored at 4 °C for future use.

Fabrication of the Gold-Modified Interdigitated Electrode. The interdigitated gold microelectrodes with 30 μm gap (Roche Company) were used for the experiments. In order to facilitate the unmodified AuNPs assembled onto the insulative gap between two neighboring comblike gold electrodes, the microgapped electrodes were sanitized, as described briefly as follows. The microgapped electrode was rinsed thoroughly with ethanol to remove possible organic contaminants, followed by immersing it in diluted piranha solution (H_2SO_4/H_2O_2 = 3:1 v/v) for 1 min and thoroughly rinsing it with ultrapure water. The cleaned microgapped electrode was immersed in ethanol containing 2.5% APTES at 4 °C for 6 h. After being rinsed thoroughly with ethanol, the microgapped electrode was dried under mild nitrogen flow and stored at 4 °C. Subsequently, the sanitized microgapped electrode was immersed in the AuNPs colloidal solution at 4 °C for 2 h and washed with ultrapure water. Then, the electrode was treated in 1 μM noncomplementary DNA for 5 min, washed with ultrapure water, and dried under mild nitrogen flow. The assembled gold nanoparticles onto the insulative gaps were characterized with a scanning electron microscope (SEM, FEI Nova NanoSEM 200).

Analytical Protocol and Measurement Procedure. The AuNPs-modified microgapped electrodes were immersed in the mixture containing the dsDNA of 1 μM probe **1** hybridized with different concentrations of target DNA and 1 μM noncomplementary DNA in 10 mM Tris−HCl and 50 mM NaCl at 30 °C. After 5 min, the electrodes were washed with ultrapure water. Subsequently, the seeded growth solution containing 150 mM glucose and 300 μM $HAuCl_4$ was applied onto the surface of the microelectrodes at 30 °C for 2 h. Subsequently, the electrodes were rinsed with ultrapure water and dried under mild nitrogen flow.

All of the electrical measurements were performed under ambient conditions in the air with a CHI electrochemical workstation (760 C, Shanghai, China). The microgapped electrode was placed in air, one pole connected to the working electrode and the other pole connected to the reference and counter electrodes. According to Ohm's law, the current through two poles of microelectrodes is proportional to the voltage applied on microelectrode arrays, with a slope equal to the electrical conductance. Thus, the electrical conductance of microelectrode arrays can be calculated immediately from $I-V$ curves obtained in linear sweep voltammetry (LSV) measurements.[21] The LSV was adopted within a potential range from −0.3 to 0.3 V with a scan rate of 1 mV/s and an interval of 1 mV.

RESULTS AND DISCUSSION

Analytical Principle of the Gap-Based Electrical Biosensor. The developed strategy relies on target DNA-induced self-catalytic growth of unmodified AuNPs as conductive bridges for amplifying DNA hybridization events, as illustrated in Scheme 1. In the assay, the insulative gap area within a pair of interdigitated microelectrodes is preliminarily modified with APTES, which facilitates unmodified AuNPs assembling onto the insulative gap area through electrostatic interaction.[14] In the presence of target DNA, probe **1** can hybridize with target DNA to form dsDNA, which cannot adsorb onto the surface of citrate-capped AuNPs assembled onto the insulative gaps due to their stable double-helix geometry and the negatively charged phosphate backbone.[17] Upon the addition of glucose and $HAuCl_4$ solution, the assembled AuNPs can catalytically oxidize glucose in the presence of O_2, producing gluconic acid and H_2O_2.[15] The obtained H_2O_2 can act as reducing agent for the reduction of $AuCl_4^-$ to Au^0 and enlarge the diameters of the assembled AuNPs,[15,22,23] resulting in a connection between most of the

dx.doi.org/10.1021/ac4032675 | Anal. Chem. 2014, 86, 1178−1185

AuNPs and a conductive gold film formation in the insulative gap. The electrons can flow through such gold films so as to form electron tunneling paths between the microelectrodes. Consequently, the conductance between microelectrodes is increased, the degree of which is correlated directly to the concentration of target DNA in the sample solution. In the absence of target DNA, ssDNA probe **1** uncoils sufficiently to expose its bases and can noncovalently bind to the assembled AuNPs,[17] resulting in the suppression of the catalytic activity sites of AuNPs. Thus, the growth of the AuNPs will not happen in glucose and $HAuCl_4$ solution, and no remarkable conductance alteration can be obtained.

Microscopy Characterization of This Sensor. In this strategy, the signal transduction mechanism is that the AuNPs with GOx-like catalytic activity assembled onto the insulative gaps exhibit different degrees of enlargement upon ssDNA and dsDNA in the solution containing glucose and $HAuCl_4$, respectively. In order to elucidate the signal transduction process, a series of solution-phase colorimetric experiments were preliminarily performed to demonstrate the fact that the GOx-like catalytic activity of AuNPs can be finely regulated by DNA hybridization. After this catalytic reaction in glucose and $HAuCl_4$ solution for 2 h, both the solution color and surface plasmon absorbance spectra for the blank sample containing ssDNA probe **1** exhibited minimum change comparing to the unmodified AuNPs with the maximum wavelength 530 nm, confirming that ssDNA adsorbed to AuNPs and blocked their catalytic activity. However, both the reaction solutions without DNA and with dsDNA color exhibited more intense red than that of the unmodified AuNPs. The surface plasmon absorbance intensities were far higher than that of the unmodified AuNPs, and the corresponding maximum wavelengths red-shifted to 542 and 546 nm, respectively (Figures S1 and S2 in the Supporting Information). These results suggested that dsDNA exhibited weaker affinity with AuNPs than ssDNA, and the unmodified AuNPs could self-catalytically grow in the reaction solution.[15,16] These samples were further characterized with TEM (Figure S3 in the Supporting Information). Upon the addition of glucose and $HAuCl_4$ solution, the spherical AuNPs with average diameter of about 20 nm were enlarged to rough, flower-like nanostructures with a relatively broad size dimension of 60−75 nm in the absence of DNA or in the presence of dsDNA, which further confirmed that the unmodified AuNPs exhibited excellent GOx-like catalytic activity and weaker affinity with dsDNA. For ssDNA probe **1** sample, the size and morphology of AuNPs remained almost unchanged. These experimental results coincided well with the reported literatures,[15,16] suggesting that GOx-like catalytic activity of AuNPs can be finely regulated by DNA hybridization, causing different catalytic growths of AuNPs in glucose and $HAuCl_4$ solution.

Scanning electron microscopy was further utilized for characterizing the morphology alteration under different solutions treatment on the AuNPs-modified insulative gap surface. For the unmodified and the APTES-modified insulative gap, there were no particles retained onto the interfaces (Figure S4, parts a and b, in the Supporting Information). After the bare AuNPs deposited onto the APTES-modified gap substrate, the large areas of interparticle distance between the AuNPs that make up the submonolayer could be clearly found from Figure 1a. Upon the addition of glucose and $HAuCl_4$, the size of assembled AuNPs became larger and a continuous gold film could be obtained (Figure 1d), indicating that the surface-

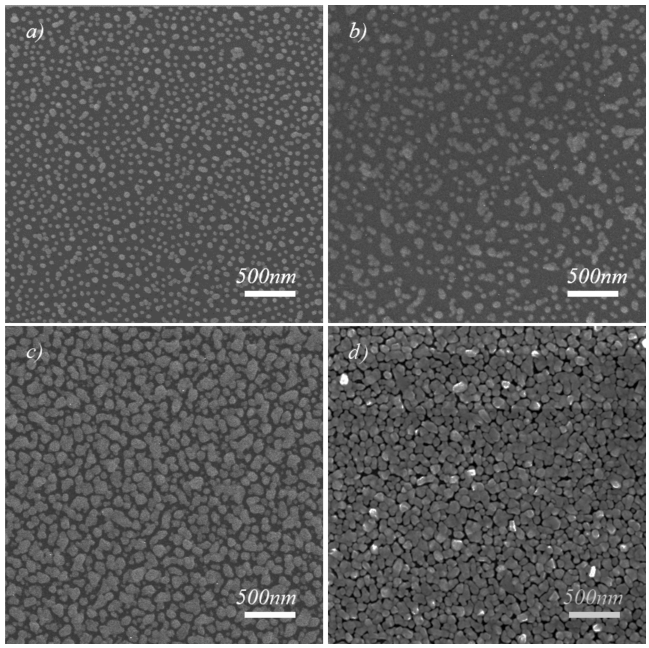

Figure 1. SEM images of bare AuNPs assembled onto APTES-modified electrodes (a), after 2 h of treatment in the solution containing 150 mM glucose and 300 μM $HAuCl_4$ for 1 μM probe **1** (b), the obtained dsDNA of 1 μM probe **1** hybridized with 1 μM target DNA (c), and the ultrapure water (d).

immobilized AuNPs exhibited excellent GOx-like catalytic activity.[15] For the control sample with only ssDNA probe **1** in the glucose and $HAuCl_4$ solution, the size of AuNPs did not become larger and the interparticle distance between AuNPs could be still visible (Figure 1b), attributing that ssDNA can fully block the catalytic activity sites of AuNPs through the noncovalent interaction between nucleotide bases of ssDNA and AuNPs.[16] In contrast, in the presence of target DNA, the size of AuNPs became larger and the neighboring AuNPs joined together, producing a continuous multilayer gold film (Figure 1c). Such gold film can facilitate the electron tunneling paths formation between the microelectrodes.

Gap-Based Electrical DNA Assay. The developed gap-based electrical DNA detection strategy was tested using a model target of hepatitis B virus (HBV)-specific DNA fragments.[24] Typical current−voltage (I−V) characteristic curves of the developed strategy are presented in Figure 2. As can be seen from Figure 2, all of the curves exhibited good linearity in the potential range, indicating that the microelectrodes behaved as ideal physical resistors under the measurement conditions.[21] For the unmodified microelectrodes, there was no appreciable current response. With the microelectrodes modified by the APTES in the insulative gap area, the current response exhibited little deviation from the unmodified electrode arrays, suggesting that APTES did not change the conductance of electrode arrays. After the assembly of citrate acid capped AuNPs onto the surface of APTES-modified gap, a slighter increasing current could be observed. Under the treatment of glucose and $HAuCl_4$, both the solution containing 1 μM ssDNA probe **1** and the control sample containing 1 μM ssDNA probe **1** and 1 μM noncomplementary DNA induced minimum current change compared to that of AuNPs-modified electrodes, suggesting that 1 μM ssDNA probe **1** could fully block the catalytic activity of AuNPs. For the dsDNA from 1 μM ssDNA probe **1** hybridized with 100

dx.doi.org/10.1021/ac4032675 | Anal. Chem. 2014, 86, 1178−1185

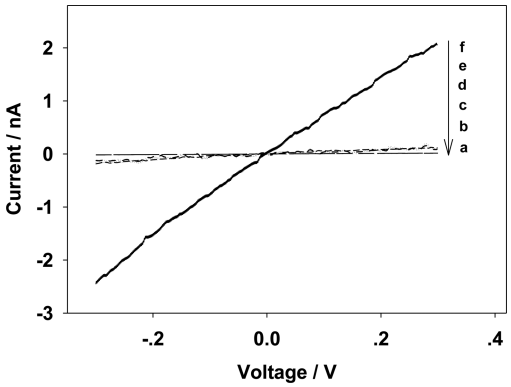

Figure 2. Representative $I-V$ curves obtained for the unmodified electrode (a), APTES-modified electrode (b), the APTES-modified electrode after 2 h of treatment in AuNPs colloids (c), the bare AuNPs-modified electrode after 2 h of treatment in 150 mM glucose and 300 μM $HAuCl_4$ solution at 30 °C for 1 μM probe **1** (d), the control sample containing 1 μM probe **1** with 1 μM non-complementary DNA (e), and the dsDNA obtained from 1 μM probe **1** hybridized with 100 pM target DNA (f). Other reaction conditions: the DNA samples adsorbed to AuNPs-modified electrodes at 30 °C for 5 min.

pM target DNA, a significantly higher current was observed at the hybridized sensor than that of the control sample, indicating that dsDNA exhibited weaker affinity with AuNPs than ssDNA, resulting in the enlargement of AuNPs and facilitating the electron transfer between the microelectrodes. However, in the absence of the initially attached AuNPs onto the electrode, there was no appreciable current response for the dsDNA from 1 μM ssDNA probe **1** hybridized with 100 pM target DNA, suggesting that the attached AuNPs can promote the reduction of $AuCl_4^-$ to Au^0 in glucose solution (Figure S5 in the Supporting Information). The $I-V$ curve of the sensor in response to 100 pM produced a large slope with an electrical conductance about 7523 pS with a standard deviation (SD) across five repetitive experiments of 21.5%, which was much greater than the approximate 415 pS (SD across five repetitive experiments of 15.5%) for the control experiment. This indicated that the developed strategy was a reliable technique with high signal-to-background ratio, excellent resistance to nonspecific detection, and high sensitivity.

Optimization of Experiment Conditions. To elucidate the possible factors which influence the conductance response characteristics of the developed strategy, further experiments were performed. In this strategy, the self-assembled time of unmodified AuNPs is quite a long related to monolayer gold film formation. The interparticles distance of AuNPs is too small to obtain excellent signal-to-background ratio for low-abundant DNA biomarkers, originating from the fact that the neighboring AuNPs can join together partly to provide the electron tunneling path, directly resulting in a sharp increase in the background current.[14] Hence, the impact of self-assembled time of bare AuNPs has been systematically investigated on the conductance of microelectrodes. As can be seen from Figure 3a, with prolonged self-assembled time of AuNPs onto the gaps, the observed conductance gradually increased and became almost leveled off at 120 min. Thus, this time was chosen as the optimized self-assembly time of AuNPs for the subsequent experiments.

Considering that the concentration of ssDNA probe **1** may be closely related to the catalytic activity of AuNPs, we further investigated the effect of the concentration of probe **1** on the conductance of microelectrodes, as shown in Figure 3b. With increased concentration of probe **1**, the observed conductance gradually decreased and reached the equilibrium at 1 μM. The obtained conductance response (435 pS, SD across five repetitive experiments of 18.9%) was compared with that of the AuNPs-modified electrodes (396 pS, SD across five repetitive experiments of 20.5%); hence, it could be supposed that 1 μM was the saturated concentration of probe **1** adsorbed to AuNPs-modified electrodes and was taken for the subsequent experiments.

In the reported AuNPs-modulating nanogap biosensors by in situ seeded growth methods, controllable growth time is necessary to improve the signal-to-background ratio.[14] So, the growth time of AuNPs in glucose and $HAuCl_4$ solution has been systematically investigated on the conductance of microelectrodes, as shown in Figure 3c. It can be found that with the increase of the growth time, the conductance response gradually increased from 30 min to 2 h, and reached the maximum at 2 h, then kept the equilibrium at 3 h. Considering that the maximum conductance response and the fact that prolonged time may enhance background response, hence, 2 h was chosen as the optimum growth time of AuNPs for the subsequent experiments.

The reported literature has demonstrated that the solution-phase AuNPs exhibit excellent GOx-like catalytic activity.[15] Hence, the concentration of glucose as GOx substrate has been systematically investigated. Figure 3d depicts the effect of the concentration of glucose on the conductance of micro-electrodes. The conductance response increased significantly as the concentration of glucose increased up to 150 mM, and then reached equilibrium at 200 mM. Next, the effect of the concentration of $HAuCl_4$ was examined, as shown in Figure 3e. The observed conductance gradually increased and became almost leveled off at 300 μM. Therefore, 150 mM and 300 μM were chosen as the optimum concentration of glucose and $HAuCl_4$ for the subsequent experiments, respectively.

The reported literatures have demonstrated that the temperature not only could influence the adsorption rate of ssDNA to AuNPs but also influence the stability of DNA duplex.[16,25] For ssDNA, with the increase of the temperature, the conductance response gradually decreased and kept the equilibrium at 30 °C (Figure S6 in the Supporting Information). However, the conductance response for dsDNA began to decrease when the temperature was above 30 °C, originating the instability of dsDNA at high temperature. Hence, 30 °C was taken as adsorption temperature of DNA on the AuNPs. Moreover, the temperature could also influence the GOx-like catalytic activity of AuNPs.[15,16] The conductance response for dsDNA increased significantly as the temperature increased up to 30 °C, and then reached equilibrium at 30 °C (Figure S7 in the Supporting Information). Hence, 30 °C was taken as catalytic reaction temperature.

Quantitative Assay of Sequence-Specific DNA. The ability of the developed biosensor strategy for quantitative assay of target DNA was investigated by immersing the AuNPs-modified microelectrodes in the solution containing 1 μM probe **1** with different concentrations of target DNA. The corresponding $I-V$ response curves are shown in Figure 4a. It can be observed that the current dynamically increased with increasing the concentration of the target DNA in the concentration range from 100 pM to 1 μM (Figure 4b depicts $I-V$ response curves for target DNA concentrations from 100

dx.doi.org/10.1021/ac4032675 | Anal. Chem. 2014, 86, 1178−1185

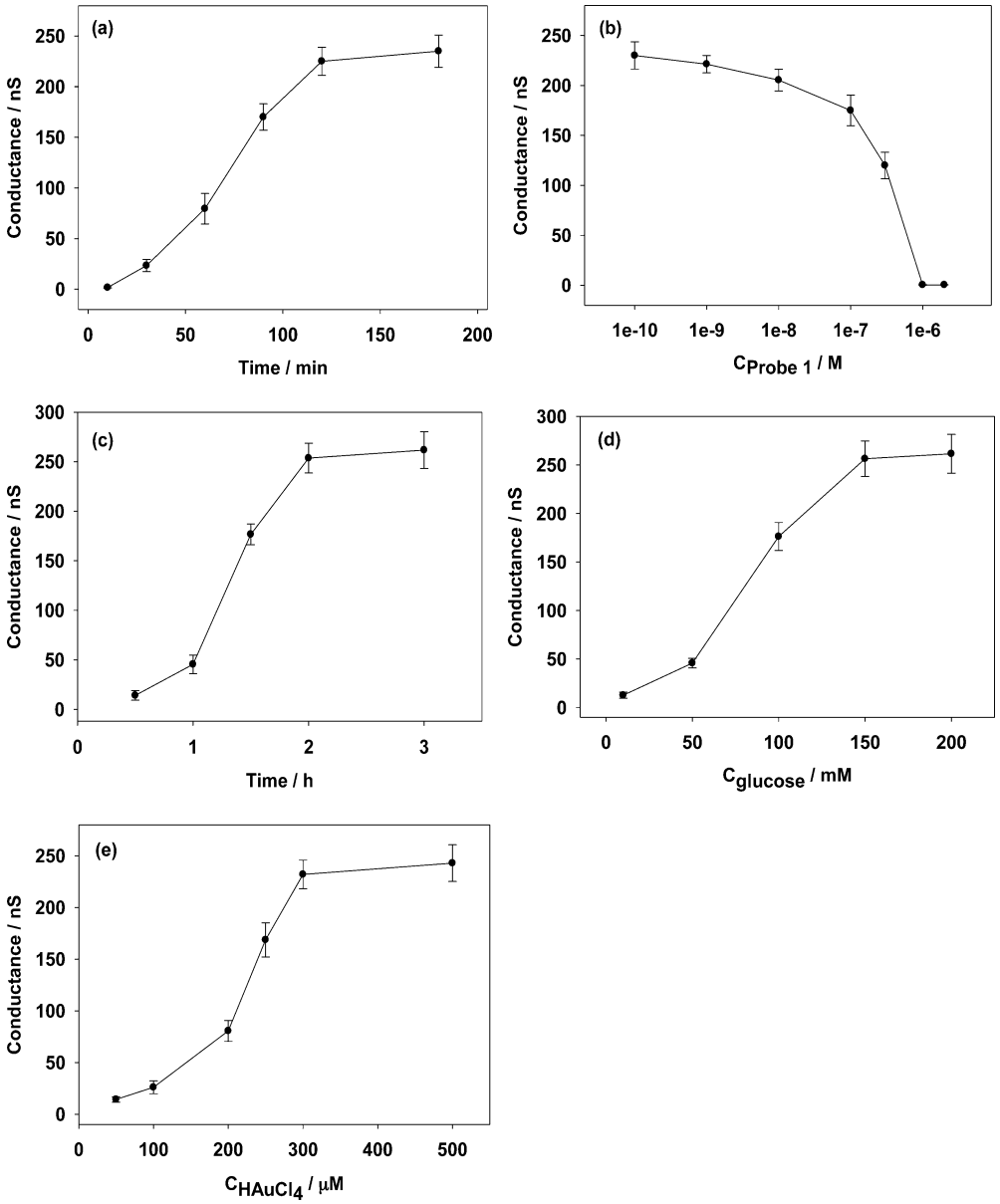

Figure 3. (a) Effect of the self-assembled time of AuNPs on the conductance response of the AuNPs-modified electrode under 150 mM glucose and 300 μM $HAuCl_4$ solution at 30 °C for 2 h for the dsDNA from 1 μM probe **1** hybridized with 1 μM target DNA. (b) Effect of the concentration of probe **1** on the conductance response of the AuNPs-modified electrode under 150 mM glucose and 300 μM $HAuCl_4$ solution at 30 °C for 2 h. (c) Effect of the growth time on the conductance response of the AuNPs-modified electrode under 150 mM glucose and 300 μM $HAuCl_4$ solution at 30 °C for the dsDNA from 1 μM probe **1** hybridized with 1 μM target DNA. (d) Effect of the glucose concentration on the conductance response of the AuNPs-modified electrode under glucose and 300 μM $HAuCl_4$ at 30 °C for 2 h for the dsDNA from 1 μM probe **1** hybridized with 1 μM target DNA. (e) Effect of the $HAuCl_4$ concentration on the conductance response of the AuNPs-modified electrode under $HAuCl_4$ and 150 mM glucose at 30 °C for 2 h for the dsDNA from 1 μM probe **1** hybridized with 1 μM target DNA. Other reaction conditions are as for Figure 2. Error bars show the standard deviation of five experiments.

pM to 3 nM), suggesting enhanced catalytic activity and enlargement degree of AuNPs at higher target DNA concentration. Most of the enlarged AuNPs can join together, facilitating a continuous multilayer gold film formation. Such gold film can promote the electron transfer between the microelectrodes and dramatically improve the current between microelectrodes. The conductance between microelectrodes in this strategy can be obtained through calculating the slopes of $I-V$ curves. The obtained conductances were used as the quantitative analytical signal for target DNA. As can be seen from Figure 4c, it can be found that a plot of the logarithm of gap conductances versus the logarithm of target DNA concentrations exhibited a good linear relationship in the concentration range from 100 pM to 1 μM with a correlation coefficient of 0.995 and a detection limit of 100 pM. These experiments results indicated that this novel gap-based electrical biosensor strategy provided superior sensitivity for the DNA detection. The superiority might be attributed to highly effective GOx-like catalytic activity and high surface differential ability of the assembled AuNPs onto the insulative gaps for ssDNA and dsDNA, which heavily altered the conductivity between microelectrodes and dramatically amplified the electrical signal for target DNA detection.

dx.doi.org/10.1021/ac4032675 | *Anal. Chem.* 2014, 86, 1178−1185

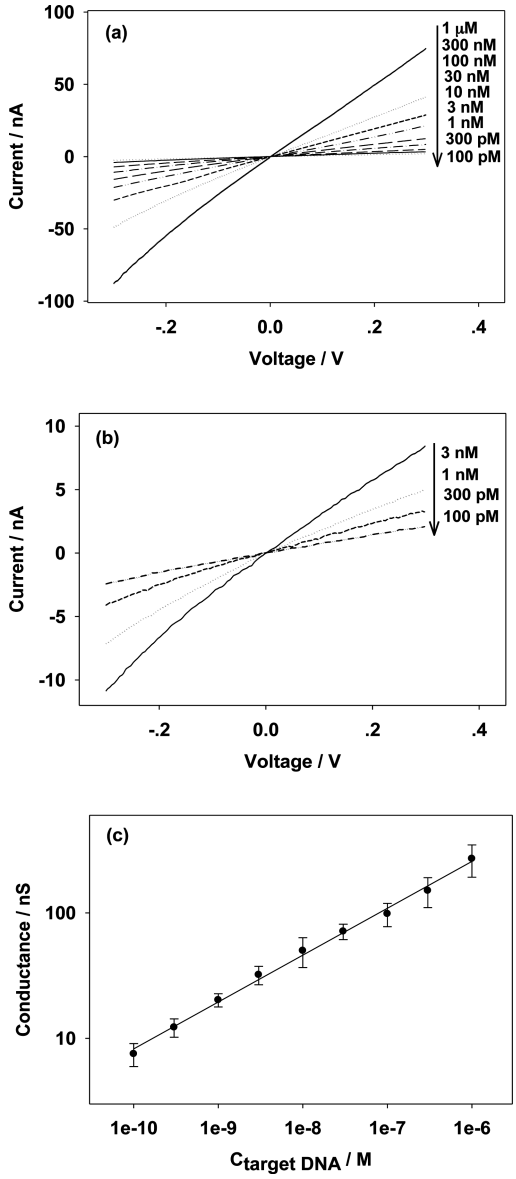

Figure 4. (a) Typical $I-V$ response curves for different target DNA concentrations from 100 pM to 1 μM. (b) $I-V$ response curves for target DNA concentrations from 100 pM to 3 nM. (c) Calibration curves of the logarithm of conductance vs the logarithm of target DNA concentration for this electrical biosensor. Other reaction conditions are as for Figure 2. Error bars show the standard deviation of five experiments.

The selectivity of this developed strategy for sequence-specific DNA assay was evaluated by using probe **1** to hybridize with the same concentration 100 pM of the complementary target DNA sequence, single-base mismatched DNA sequence and two-base mismatch DNA sequence, respectively. In real biological samples, there was a large excess of noncomplementary DNA with long fragments coexisting with target DNA. Hence, the solution containing 1 μM noncomplementary DNA with long fragment (100 nucleotides) was used as the control sample. Measurement for ultrapure water in place of the complementary DNA was used as the blank sample (Figure S8 in the Supporting Information). The conductance responses for the 100 pM mismatched DNA are slightly higher than that of the control sample and the blank sample. However, both the target DNA and the mixture solution containing target DNA and noncomplementary DNA yielded significantly higher conductivity responses than that of the control sample. These results indicated that the developed assay strategy exhibited high specificity to discriminate the perfectly matched sequence from the mismatched sequences.

CONCLUSIONS

We have developed a novel gap-electrical biosensor strategy for DNA hybridization detection based on self-catalytic growth of unmodified AuNPs as conductive bridges mediated electrical signal transduction. This strategy exploited the variation of the GOx-like catalytic activity of AuNPs upon interaction with ssDNA and dsDNA, which induced different degrees of enlargement of the assembled AuNPs on the insulative gap in the solution containing glucose and $HAuCl_4$ with concomitant modulation of the conductivity alteration between microelectrodes, respectively. The experimental results revealed that this strategy exhibited dynamic responses to the target DNA with a low detection limit. Moreover, this sensor afforded high selectivity for target DNA against mismatched DNA. We noted that this developed strategy could not simultaneously measure multiple analytes in a single run. However, it is possible to utilize multiple microelectrodes arrays to simultaneously measure multiple analytes. Moreover, the developed strategy may be applied in biological fluids under sample separation in order to prevent from the strong protein adsorption.

ASSOCIATED CONTENT

Supporting Information

Description of other experimental procedures and additional figures. This material is available free of charge via the Internet at http://pubs.acs.org.

AUTHOR INFORMATION

Corresponding Authors

*E-mail: huaguinie@126.com. Phone: 86-577-88373017. Fax: 86-577-88373017.

*E-mail: smhuang@wzu.edu.cn. Phone: 86-577-88373017. Fax: 86-577-88373017.

Notes

The authors declare no competing financial interest.

ACKNOWLEDGMENTS

This work was supported in part by grants from NSFC (21005055, 21273163, 51002106, and 21173159), NSFZJ (LY13B050002, LQ12E02005), ZJST (2012R10014-09), NSFC for Distinguished Young Scholars (51025207), Open Foundation of State Key Laboratory of Chemo/Bio-Sensing and Chemometrics (2012005), and Xinmiao talent project of Zhejiang Province (2012R424053).

REFERENCES

(1) Sassolas, A.; Leca-Bouvier, B. D.; Blum, L. J. *Chem. Rev.* **2008**, *108*, 109−139.

(2) Nie, H. G.; Yang, Z.; Huang, S. M.; Wu, Z.; Wang, H. Q.; Yu, R. Q.; Jiang, J. H. *Small* **2012**, *8*, 1407−1414.

(3) Kutyavin, I. *Nucleic Acids Res.* **2010**, *38*, e29.

(4) Crane, B. L.; Hogan, N. C.; Sudo, H.; Thilly, W. G.; Hunter, I. W. *Anal. Chem.* **2005**, *77*, 5129−5134.

(5) Chen, X.; Guo, Z.; Yang, G. M.; Li, J.; Li, J. H.; Huang, X. J. *Mater. Today* **2010**, *13*, 28−41.

(6) Roy, S.; Gao, Z. Q. *Nano Today* **2009**, *4*, 318−334.

(7) Saha, K.; Agasti, S. S.; Kim, C.; Li, X. N.; Rotello, V. M. *Chem. Rev.* **2012**, *112*, 2739−2779.
(8) Park, S. J.; Taton, T. A.; Mirkin, C. A. *Science* **2002**, *295*, 1503−1506.
(9) Nam, J. M.; Thaxton, C. S.; Mirkin, C. A. *Science* **2003**, *301*, 1884−1886.
(10) Stoeva, S. I.; Lee, J. S.; Thaxton, C. S.; Mirkin, C. A. *Angew. Chem., Int. Ed.* **2006**, *45*, 3303−3306.
(11) Tokonami, S.; Shiigi, H.; Nagaoka, T. *Anal. Chem.* **2008**, *80*, 8071−8075.
(12) Fang, C.; Fan, Y.; Kong, J.; Gao, Z.; Balasubramanian, N. *Anal. Chem.* **2008**, *80*, 9387−9394.
(13) Chen, C. C.; Ko, F. H.; Chen, C. T.; Liu, T. F.; Chang, E. Y.; Yang, Y. S.; Yan, S. J.; Chu, T. C. *Appl. Phys. Lett.* **2007**, *91*, 2531031−2531033.
(14) Yu, Y.; Chen, X.; Wei, Y.; Liu, J. H.; Yu, S. H.; Huang, X. J. *Small* **2012**, *8*, 3274−3284.
(15) Luo, W. J.; Zhu, C. F.; Su, S.; Li, D.; He, Y.; Huang, Q.; Fan, C. H. *ACS Nano* **2010**, *4*, 7451−7458.
(16) Zheng, X. X.; Liu, Q.; Jing, C.; Li, Y.; Li, D.; Luo, W. J.; Wen, Y. Q.; He, Y.; Huang, Q.; Long, Y. T.; Fan, C. H. *Angew. Chem., Int. Ed.* **2011**, *50*, 11994−11998.
(17) Li, H.; Rothberg, L. J. *Proc. Natl. Acad. Sci. U.S.A.* **2004**, *101*, 14036−14039.
(18) Zhao, W.; Brook, M. A.; Li, Y. F. *ChemBioChem* **2008**, *9*, 2363−2371.
(19) Song, Y. J.; Wei, W. L.; Qu, X. G. *Adv. Mater.* **2011**, *23*, 4215−4236.
(20) Zhen, Z.; Tang, L. J.; Long, H. X.; Jiang, J. H. *Anal. Chem.* **2012**, *84*, 3614−3620.
(21) Huang, Y.; Wang, T. H.; Jiang, J. H.; Shen, G. L.; Yu, R. Q. *Clin. Chem.* **2009**, *55*, 964−971.
(22) Rica, R. D. I.; Stevens, M. M. *Nat. Nanotechnol.* **2012**, *7*, 821−824.
(23) Lorenzo, L. R.; Rica, R. D. I.; Puebla, R. A. A.; Marzan, L. M. L.; Stevens, M. M. *Nat. Mater.* **2012**, *11*, 604−607.
(24) Ariksoysal, D. O.; Karadeniz, H.; Erdem, A.; Sengonul, A.; Sayiner, A. A.; Ozsoz, M. *Anal. Chem.* **2005**, *77*, 4908−4917.
(25) Li, H.; Rothberg, L. J. *J. Am. Chem. Soc.* **2004**, *126*, 10958−10961.